PERGAMON

International Journal of Solids and Structures 39 (2002) 5699–5717

INTERNATIONAL JOURNAL OF SOLIDS and STRUCTURES

www.elsevier.com/locate/ijsolstr

The nonlinear viscoelastic response of carbon black-filled natural rubbers

Aleksey D. Drozdov [a,*], Al Dorfmann [b]

[a] *Department of Production, Aalborg University, Fibigerstraede 16, DK–9220 Aalborg, Denmark*
[b] *Institute of Structural Engineering, 82 Peter Jordan Street, A-1190 Vienna, Austria*

Received 29 January 2002; received in revised form 29 July 2002

Abstract

Three series of tensile relaxation tests are performed on natural rubber filled with various amounts of carbon black. The elongation ratio varies in the range from $\lambda = 2.0$ to 3.5. Constitutive equations are derived for the nonlinear viscoelastic behavior of filled elastomers. Applying a homogenization method, we model a particle-reinforced rubber as a transient network of macromolecules bridged by junctions (physical and chemical cross-links, entanglements and filler clusters). The network is assumed to be strongly heterogeneous at the meso-level: it consists of passive regions, where rearrangement of chains is prevented by surrounding macromolecules and filler particles, and active domains, where active chains separate from temporary nodes and dangling chains merge with the network as they are thermally agitated. The rate of rearrangement obeys the Eyring equation, where different active meso-domains are characterized by different activation energies. Stress–strain relations for a particle-reinforced elastomer are derived by using the laws of thermodynamics. Adjustable parameters in the constitutive equations are found by fitting experimental data. It is demonstrated that the filler content strongly affects the rearrangement process: the attempt rate for separation of strands from temporary nodes increases with elongation ratio at low fractions of carbon black (below the percolation threshold) and decreases with λ at high concentrations of filler.

Keywords: Nonlinear; Viscoelastic; Rubbers; Elastomers

1. Introduction

This paper is concerned with the viscoelastic behavior of carbon black-filled rubbers at isothermal loading with finite strains. The time-dependent response of particle-reinforced elastomers (rubbery polymers filled with carbon black or silica and solid propellants reinforced by rigid particles) has been a focus of attention in the past five years (Aksel and Hübner, 1996; Holzapfel and Simo, 1996; Lion, 1996, 1997, 1998; Spathis, 1997; Bergström and Boyce, 1998; Ha and Schapery, 1998; Reese and Govindjee, 1998; Septanika and Ernst, 1998a,b; Clarke et al., 2000; Jung et al., 2000; Miehe and Keck, 2000; Wu and Liechti, 2000;

* Corresponding author. Tel.: +45-9635-8938; fax: +45-9815-3030.
E-mail address: drozdov@iprod.auc.dk (A.D. Drozdov).

0020-7683/02/$ - see front matter © 2002 Elsevier Science Ltd. All rights reserved.
PII: S0020-7683(02)00455-9

Boukamel et al., 2001; Haupt and Sedlan, 2001; Kim and Youn, 2001; Drozdov and Dorfmann, 2002). This may be explained by numerous applications of these materials in industry (vehicle tires, shock absorbers, earthquake bearings, seals, flexible joints, solid propellants, etc.).

The objective of this study is three-fold:

1. To report experimental data in tensile relaxation tests on rubber compounds with various contents of filler.
2. To derive constitutive equations for the time-dependent response of a particle-reinforced elastomer at finite strains.
3. To assess the influence of filler fraction on the viscoelastic behavior of filled rubbers by fitting experimental data at several elongation ratios.

The time-dependent response of a filled rubber is described by using the concept of transient networks (Green and Tobolsky, 1946; Yamamoto, 1956; Tanaka and Edwards, 1992). A complicated micro-structure of a rubber compound is modelled as an equivalent heterogeneous network of macromolecules. The network is treated as an ensemble of meso-regions with various potential energies for separation of active chains from temporary nodes and attachment of dangling chains to the network junctions (physical and chemical cross-links, entanglements and aggregates of filler).

The following features distinguish the present model from previous studies on the viscoelastic behavior of temporary networks, see, e.g., Tanaka and Edwards (1992); Drozdov (1997) and Septanika and Ernst (1998a,b):

1. The ensemble of meso-regions is split into two types of domains: (i) active, where rearrangement of chains is governed by the Eyring equation for thermally activated processes, and passive, where separation of chains from temporary junctions is prevented by surrounding macromolecules and aggregates of filler.
2. The distribution of activation energies for detachment of chains from the network is described by the random energy model with adjustable parameters independent of mechanical factors.
3. The attempt rate for separation of chains from temporary nodes and the concentration of strands in active meso-regions are assumed to be strongly affected by strain. The number of active strands in the transient network increases and the number of passive strands decreases under stretching.

The exposition is organized as follows. The specimens and the experimental procedure are described in Section 2. A micro-mechanical model for a filled elastomer is proposed in Section 3. Kinetic equations for separation of active strands from temporary junctions are developed in Section 4. Stress–strain relations are derived in Section 5 by using the laws of thermodynamics. Uniaxial extension of a specimen is analyzed in Section 6. Adjustable parameters in the constitutive equations are determined in Section 7 by fitting observations. A brief discussion of our findings is given in Section 8. The present approach is compared with other models for the time-dependent behavior of disordered media in Section 9. Some concluding remarks are formulated in Section 10.

2. Experimental procedure

Three series of uniaxial tensile relaxation tests were performed at room temperature. ASTM dumbbell specimens for the first series of tests with overall length 90 mm and width 4 mm and thickness 1 mm in the active zone were provided by TARRC laboratories (UK). The fraction of carbon black (CB) was 45 phr (parts per hundred parts of rubber) by weight. These samples were designated as R1. ASTM dumbbell

specimens for the other two series of experiments with overall length 90 mm and width 4 mm and thickness 2 mm in the active zone were supplied by Semperit (Austria). The fraction of CB in these samples was 20 and 60 phr. These specimens were designated as R2 (20 phr) and R3 (60 phr).

It is assumed by the suppliers that the filler content in rubbery compounds R1 and R2 is below the percolation threshold, which means that filler particles aggregate in isolated clusters only, whereas the fraction of carbon black in compound R3 exceeds the threshold, which results in the formation of a secondary network of filler.

Relaxation tests were performed on a testing machine designed at the Institute of Physics (Vienna, Austria). The devise was equipped by a video-controlling system. To measure the longitudinal strain, two reflection lines were drawn in the central part of each specimen before loading (with the distance 7 mm between them). Changes in the distance between these lines were measured by a video-extensometer. The tensile force was measured by using a standard load cell. The engineering stress, σ_e, was determined as the ratio of the axial force to the cross-sectional area of a specimen in the stress-free state.

All samples were used as received without thermal pre-treatment. In any test, a specimen was elongated with a constant rate of engineering strain $\dot{\epsilon} = 1.33 \times 10^{-2}\ s^{-1}$ up to a given elongation ratio λ. According to Arruda et al. (1995) and Inberg et al. (2002), loading with this strain rate provides nearly isothermal test conditions. Afterwards, the strain was preserved constant during the relaxation time $t_r = 1$ h. This time slightly exceeds the standard duration of relaxation tests (10^3 s), but it is substantially less than the characteristic time for stress-induced aging of rubbers (driven by isomerisation of sulphur cross-links (Clarke et al., 2000) or mechanically induced diffusion of anti-degradants (Choi, 1998, 2002)).

Each test was performed on a new specimen. Relaxation curves at four elongation ratios, $\lambda_1 = 2.0$, $\lambda_2 = 2.5$, $\lambda_3 = 3.0$, $\lambda_4 = 3.5$, are depicted in Figs. 1–3. In these figures the engineering stress, σ_e, is plotted versus the logarithm ($\log = \log_{10}$) of time t (the initial instant $t = 0$ corresponds to the beginning of a relaxation test).

Figs. 1–3 demonstrate that the stress, σ_e, monotonically increases with elongation ratio, λ, and the shape of the relaxation curves is noticeably altered by strain. To compare the relaxation curves quantitatively, we develop a constitutive model for the viscoelastic response of particle-reinforced rubbers at finite strains.

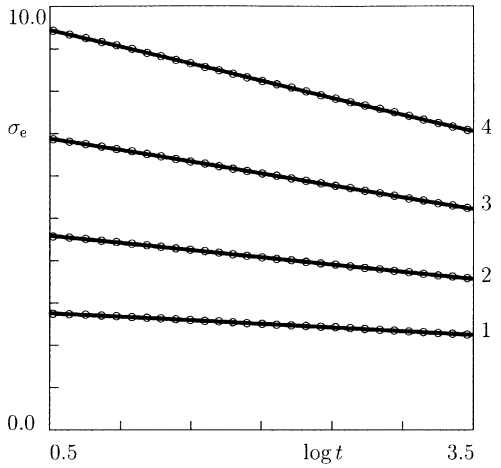

Fig. 1. The engineering stress σ_e MPa versus time t s in a tensile relaxation test with an elongation ratio λ. Circles: experimental data for specimens R1. Solid lines: results of numerical simulation. Curve 1: $\lambda = 2.0$; curve 2: $\lambda = 2.5$; curve 3: $\lambda = 3.0$; curve 4: $\lambda = 3.5$.

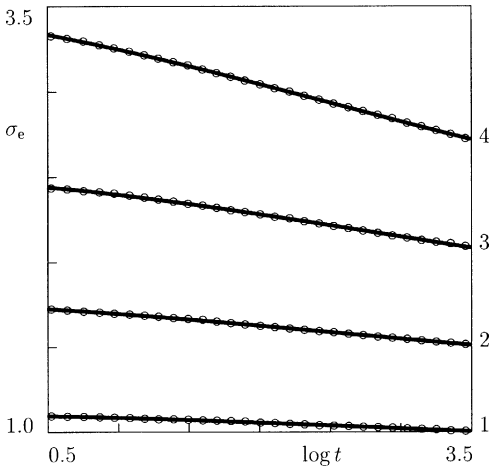

Fig. 2. The engineering stress σ_e MPa versus time t s in a tensile relaxation test with an elongation ratio λ. Circles: experimental data for specimens R2. Solid lines: results of numerical simulation. Curve 1: $\lambda = 2.0$; curve 2: $\lambda = 2.5$; curve 3: $\lambda = 3.0$; curve 4: $\lambda = 3.5$.

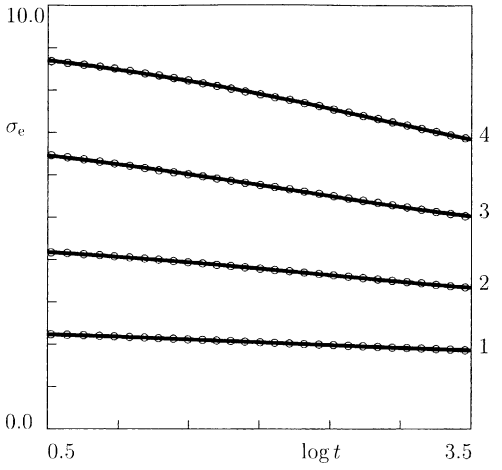

Fig. 3. The engineering stress σ_e MPa versus time t s in a tensile relaxation test with an elongation ratio λ. Circles: experimental data for specimens R3. Solid lines: results of numerical simulation. Curve 1: $\lambda = 2.0$; curve 2: $\lambda = 2.5$; curve 3: $\lambda = 3.0$; curve 4: $\lambda = 3.5$.

3. A micro-mechanical model

A particle-reinforced elastomer is a composite medium consisting of particles of filler and their aggregates randomly distributed in the host material. The average size of carbon black clusters ranges from several tens to hundreds of nanometers. During preparation of specimens (at the stages of mixing and vulcanization) three processes take place in filled elastomers:

1. Formation of a secondary network of filler when the content of reinforcement exceeds some threshold value (Karasek and Sumita, 1996).

2. Segregation of short chains to the interfaces between the aggregates of filler and the host matrix, which results in a pronounced decrease in the concentration of junctions in the bulk elastomer, where short chains serve as physical cross-links (Carlier et al., 2001).
3. Formation of glass-like hard cores around particles and their aggregates (Karasek and Sumita, 1996; Mandal and Aggarwal, 2001).

Under stretching, a particle-reinforced rubber suffers substantial changes in its micro-structure:

1. Large clusters of filler and the secondary network break-down into pieces, which leads to release of occluded rubber (a part of the elastomeric matrix whose deformation is screened by surrounding particles at relatively small strains).
2. Polymeric chains slide along and detach from particles, which results in destruction of rigid cores surrounding clusters of filler and creation of vacuoles.
3. Interactions between macromolecules in the host material are weakened, which leads to acceleration of stress relaxation, on the one hand, and formation of voids in the host matrix, on the other.
4. Severe straining results in orientation of chains in the direction of maximal stresses and mechanically induced crystallization of macromolecules.

It is hard to believe that these transformations of morphology can be adequately described by a constitutive model with a small number of adjustable parameters. To develop stress–strain relations, we apply a method of "homogenization of micro-structure" (Bergström et al., 2002). According to this concept, an equivalent phase is introduced whose deformation captures essential features of the response of a filled elastomer. To analyze the viscoelastic behavior of a particle-reinfoced rubber, we accept a transient network of macromolecules as the equivalent phase. This approach ascribes the time-dependent response of filled elastomers to rearrangement of chains in the elastomeric matrix (which, in turn, is substantially affected by the distribution of filler).

The network is assumed to be strongly inhomogeneous, and it is treated as an ensemble of meso-regions with various strengths of inter-chain interactions. The characteristic length of a meso-region is estimated as several micrometers that substantially exceeds the radius of gyration for a macromolecule and the average diameter for a filler cluster, on the one hand, and that is noticeably less than a size of a specimen, on the other. The heterogeneity of the network is formed at the stage of preparation of specimens, and it is attributed to a spatial inhomogeneity in the distributions of a cross-linker and filler particles.

The network is split into two types of meso-regions: (i) passive, where inter-chain interaction prevents separation of chains from their junctions, and (ii) active, where active strands (whose ends are bridged to contiguous junctions) separate from the temporary nodes and dangling strands capture nearby junctions at random times when they are thermally agitated.

Denote by N_p the number of strands (per unit mass) in passive meso-domains and by N_a the number of active strands (per unit mass) in active meso-regions. Deformation of the network induces (i) weakening of inter-chain interactions at active loading, which results in an increase in the number of active meso-regions, and (ii) strengthening of interactions between macromolecules at unloading, which implies that rearrangement of strands in some active meso-domains becomes prevented by surrounding chains. For an arbitrary loading process, the quantities N_a and N_p are treated as functions of time which obey the conservation law

$$N_a(t) + N_p(t) = N, \tag{1}$$

where N is the total number (per unit mass) of active strands in active and passive meso-regions. We suppose that N is independent of mechanical factors.

Rearrangement of a temporary network in active meso-domains is treated as a thermally activated process, whose rate obeys the Eyring equation (Eyring, 1936). In a stress-free medium, the rate of separation of an active strand from a junction in an active meso-region with potential energy $\bar{\omega}$ is given by

$$\Gamma(\bar{\omega}) = \Gamma_0 \exp\left(-\frac{\bar{\omega}}{k_B T}\right),$$

where $\bar{\omega}$ is the activation energy for detachment of strands, k_B is Boltzmann's constant, and the pre-factor Γ_0 is independent of temperature. Introducing the dimensionless energy for separation,

$$\omega = \frac{\bar{\omega}}{k_B T_0},$$

where T_0 is some reference temperature, and disregarding the influence of small increments of temperature, $\Delta T = T - T_0$, on the attempt rate, Γ_0, we present the Eyring equation as follows:

$$\Gamma(\omega) = \Gamma_0 \exp(-\omega). \tag{2}$$

In what follows, we suppose that Eq. (2) remains valid for an arbitrary loading process, provided that the attempt rate, Γ_0, is a function of the current strain.

The distribution of active strands in active meso-regions is determined by the probability density $p(\omega)$: the quantity $N_a(t)p(\omega)\,d\omega$ equals the current number of active strands (per unit mass) whose potential energies for separation, ω', belong to the interval $[\omega, \omega + d\omega]$.

4. Rearrangement of active strands

Detachment of active strands from temporary nodes and merging of dangling strands with the network are entirely described by the function $n(t, \tau, \omega)$ that equals the number (per unit mass) of active strands at time t in active meso-regions with potential energy ω which have last been bridged to the network before instant $\tau \in [0, t]$.

The quantity $n(t, t, \omega)$ equals the number of active strands (per unit mass) with the energy for separation ω at time t,

$$n(t, t, \omega) = N_a(t)p(\omega). \tag{3}$$

The function

$$\gamma(\tau, \omega) = \frac{\partial n}{\partial \tau}(t, \tau, \omega)\bigg|_{t=\tau} \tag{4}$$

is the rate of reformation for dangling chains: the amount $\gamma(\tau, \omega)\,d\tau$ equals the number of dangling strands (per unit mass) in active regions with potential energy ω that merge with the temporary network within the interval $[\tau, \tau + d\tau]$. The quantity

$$\frac{\partial n}{\partial \tau}(t, \tau, \omega)\,d\tau$$

is the number of these strands that have not detached during the interval $[\tau, t]$. The amount

$$-\frac{\partial n}{\partial t}(t, 0, \omega)\,dt$$

is the number of active strands (per unit mass) that separate (for the first time) from the network within the interval $[t, t + dt]$. Finally, the quantity

$$-\frac{\partial^2 n}{\partial t \partial \tau}(t,\tau,\omega)\,\mathrm{d}t\,\mathrm{d}\tau$$

is the number of strands (per unit mass) that have last been linked to the network within the interval $[\tau, \tau+\mathrm{d}\tau]$ and separate from the network (for the first time after merging) during the interval $[t, t+\mathrm{d}t]$.

The rate of separation, Γ, is determined as the ratio of the number of active strands detaching from temporary nodes per unit time to the total number of active strands. Applying this definition to active strands merging with the network within the interval $[\tau, \tau+\mathrm{d}\tau]$, we arrive at the differential equation

$$\frac{\partial^2 n}{\partial t \partial \tau}(t,\tau,\omega) = -\Gamma(t,\omega)\frac{\partial n}{\partial \tau}(t,\tau,\omega), \tag{5}$$

where the first argument of the function $\Gamma(t,\omega)$ accounts for the effect of time-dependent strain on the attempt rate Γ_0 in Eq. (2).

Rearrangement of strands linked to temporary junctions in the stress-free state is governed by the following processes:

1. Thermally activated detachment of active strands from temporary nodes.
2. Stress-induced activation of passive meso-regions under active loading.

Evolution of the function $n(t,0,\omega)$ is described by the kinetic equation

$$\frac{\partial n}{\partial t}(t,0,\omega) = -\Gamma(t,\omega)n(t,0,\omega) - \frac{\mathrm{d}N_\mathrm{p}}{\mathrm{d}t}(t)p(\omega). \tag{6}$$

Integration of Eqs. (5) and (6) with initial conditions (3) (where we set $t=0$) and (4) implies that

$$n(t,0,\omega) = \left\{N_\mathrm{a}(0)\exp\left[-\int_0^t \Gamma(s,\omega)\,\mathrm{d}s\right] - \int_0^t \frac{\mathrm{d}N_\mathrm{p}}{\mathrm{d}t}(\tau)\exp\left[-\int_\tau^t \Gamma(s,\omega)\,\mathrm{d}s\right]\mathrm{d}\tau\right\}p(\omega), \tag{7}$$

$$\frac{\partial n}{\partial \tau}(t,\tau,\omega) = \gamma(\tau,\omega)\exp\left[-\int_\tau^t \Gamma(s,\omega)\,\mathrm{d}s\right]. \tag{8}$$

To exclude the function $\gamma(t,\omega)$ from Eq. (8), we use the identity

$$n(t,t,\omega) = n(t,0,\omega) + \int_0^t \frac{\partial n}{\partial \tau}(t,\tau,\omega)\,\mathrm{d}\tau.$$

Substitution of expressions (3), (7) and (8) into this equality results in

$$N_\mathrm{a}(t)p(\omega) = \left\{N_\mathrm{a}(0)\exp\left[-\int_0^t \Gamma(s,\omega)\,\mathrm{d}s\right] - \int_0^t \frac{\mathrm{d}N_\mathrm{p}}{\mathrm{d}t}(\tau)\exp\left[-\int_\tau^t \Gamma(s,\omega)\,\mathrm{d}s\right]\mathrm{d}\tau\right\}p(\omega) + \int_0^t \gamma(\tau,\omega)\exp\left[-\int_\tau^t \Gamma(s,\omega)\,\mathrm{d}s\right]\mathrm{d}\tau. \tag{9}$$

The solution of the integral equation (9) together with Eq. (1) reads

$$\gamma(t,\omega) = N_\mathrm{a}(t)\Gamma(t,\omega)p(\omega).$$

It follows from this equality and Eq. (8) that

$$\frac{\partial n}{\partial \tau}(t,\tau,\omega) = N_\mathrm{a}(\tau)\Gamma(\tau,\omega)p(\omega)\exp\left[-\int_\tau^t \Gamma(s,\omega)\,\mathrm{d}s\right]. \tag{10}$$

5. Constitutive equations

We adopt conventional assumptions that (i) the excluded-volume effect and other multi-chain effects are screened for an individual chain by surrounding macromolecules, and (ii) the energy of interaction between strands can be taken into account with the help of the incompressibility condition (Tanaka and Edwards, 1992). We also accept the affinity hypothesis that disregards thermal oscillations of junctions and presumes that the deformation gradient for the motion of junctions at the micro-level coincides with the deformation gradient for the motion of appropriate points of an elastomer at the macro-level (Yamamoto, 1956).

At isothermal deformation, meso-regions in the network are treated as isotropic incompressible media. The strain energy per strand in a passive meso-domain, $\bar{w}$, is assumed to depend on the first two principal invariants I_k $(k = 1, 2)$ of the right Cauchy tensor, $\mathbf{C}_0(t)$, for transition from the reference state to the deformed state at time t,

$$\bar{w}(t) = w(I_1(\mathbf{C}_0(t)), I_2(\mathbf{C}_0(t))).$$

A conventional hypothesis is accepted that stress in a dangling strand totally relaxes before this strand captures a new junction (Tanaka and Edwards, 1992). This implies that the stress-free state of an active strand that merges with the network at time $\tau \geqslant 0$ coincides with the deformed state of the network at that instant. The strain energy, $\bar{w}_0(t, 0)$, of an active strand that has not separated from the network during the interval $[0, t]$, depends on the first two principal invariants of the right Cauchy tensor $\mathbf{C}_0(t)$,

$$\bar{w}_0(t, 0) = w(I_1(\mathbf{C}_0(t)), I_2(\mathbf{C}_0(t))).$$

For an active strand that has last been reformed at time $\tau \in [0, t]$,

$$\bar{w}_0(t, \tau) = w(I_1(\mathbf{C}(t, \tau)), I_2(\mathbf{C}(t, \tau))),$$

where $\mathbf{C}(t, \tau)$ is the relative right Cauchy tensor for transition from the deformed state at instant τ to the deformed state at time $t \geqslant \tau$. The same function, w, is used to describe strain energies of strands in various meso-domains, which is assumed to vanish in the reference state,

$$w(I_1, I_2)|_{I_1=3, I_2=3} = 0. \tag{11}$$

We do not dwell on an explicit expression for the function w. For a survey of strain energy densities of rubber-like materials, the reader is referred to recent reviews by Boyce and Arruda (2000) and Kloczkowski (2002).

Confining ourselves to active loading processes (i.e., excluding from the consideration transition of active meso-domains into the passive state driven by mechanical factors), we sum the mechanical energies of strands in passive meso-domains and those of active strands in active meso-regions (that merged with the network at various times $\tau \in [0, t]$), and find the strain energy density per unit mass of an elastomer

$$\begin{aligned} W(t) = {} & \left[N_{\mathrm{p}}(t) + \int_0^\infty n(t, 0, \omega)\, \mathrm{d}\omega \right] w(I_1(\mathbf{C}_0(t)), I_2(\mathbf{C}_0(t))) \\ & + \int_0^t \left[\int_0^\infty \frac{\partial n}{\partial \tau}(t, \tau, \omega)\, \mathrm{d}\omega \right] w(I_1(\mathbf{C}(t, \tau)), I_2(\mathbf{C}(t, \tau)))\, \mathrm{d}\tau. \end{aligned} \tag{12}$$

Differentiating Eq. (12) with respect to time and using Eqs. (5), (6) and (11), we obtain

$$\frac{\mathrm{d}W}{\mathrm{d}t}(t) = V(t) + U(t) - Y(t), \tag{13}$$

where

$$
\begin{aligned}
V(t) &= \left[N_{\mathrm{p}}(t) + \int_0^\infty n(t,0,\omega)\,\mathrm{d}\omega\right]\left[\frac{\partial w}{\partial I_1}(I_1(\mathbf{C}_0(t)),I_2(\mathbf{C}_0(t)))\frac{\mathrm{d}I_1}{\mathrm{d}t}(\mathbf{C}_0(t))\right.\\
&\quad\left.+\frac{\partial w}{\partial I_2}(I_1(\mathbf{C}_0(t)),I_2(\mathbf{C}_0(t)))\frac{\mathrm{d}I_2}{\mathrm{d}t}(\mathbf{C}_0(t))\right],\\
U(t) &= \int_0^t\left[\int_0^\infty \frac{\partial n}{\partial\tau}(t,\tau,\omega)\,\mathrm{d}\omega\right]\left[\frac{\partial w}{\partial I_1}(I_1(\mathbf{C}(t,\tau)),I_2(\mathbf{C}(t,\tau)))\frac{\partial I_1}{\partial t}(\mathbf{C}(t,\tau))\right.\\
&\quad\left.+\frac{\partial w}{\partial I_2}(I_1(\mathbf{C}(t,\tau)),I_2(\mathbf{C}(t,\tau)))\frac{\partial I_2}{\partial t}(\mathbf{C}(t,\tau))\right]\mathrm{d}\tau,\\
Y(t) &= \left[\int_0^\infty \Gamma(t,\omega)n(t,0,\omega)\,\mathrm{d}\omega\right]w(I_1(\mathbf{C}_0(t)),I_2(\mathbf{C}_0(t)))\\
&\quad+\int_0^t\left[\int_0^\infty \Gamma(t,\omega)\frac{\partial n}{\partial\tau}(t,\tau,\omega)\,\mathrm{d}\omega\right]w(I_1(\mathbf{C}(t,\tau)),I_2(\mathbf{C}(t,\tau)))\,\mathrm{d}\tau.
\end{aligned}
\tag{14}
$$

The functions $n(t,0,\omega)$ and $\partial n/\partial\tau(t,\tau,\omega)$ are non-negative: they stand for the number (per unit mass) of active strands that have not been detached from the network during the interval $[0,t]$ and for the number (per unit mass) of strands merged with the network at instant $\tau\in[0,t]$ and remaining active up to time t, respectively. Because the rate of breakage of active chains, Γ, and the potential energy per chain, w, are also non-negative (the latter follows from Eq. (11)), the last equality in Eq. (14) implies that the function $Y(t)$ is non-negative for an arbitrary deformation program.

The derivatives of the principal invariants, I_k ($k=1,2$), of the relative right Cauchy tensor are given by (Drozdov, 1996)

$$
\begin{aligned}
&\frac{\partial I_1}{\partial t}(\mathbf{C}(t,\tau)) = 2\mathbf{B}(t,\tau):\mathbf{D}(t),\\
&\frac{\partial I_2}{\partial t}(\mathbf{C}(t,\tau)) = 2\left[I_1(\mathbf{C}(t,\tau))\mathbf{B}(t,\tau)-\mathbf{B}^2(t,\tau)\right]:\mathbf{D}(t),
\end{aligned}
\tag{15}
$$

where $\mathbf{B}(t,\tau)$ is the relative left Cauchy tensor for transition from the deformed state at time τ to the deformed state at time t, $\mathbf{D}(t)$ is the rate-of-strain tensor, and the colon stands for convolution of tensors. Substitution of expressions (15) into Eq. (14) implies that

$$
U(t) = 2\boldsymbol{\Lambda}(t):\mathbf{D}(t),
\tag{16}
$$

where

$$
\boldsymbol{\Lambda}(t) = \int_0^t\left[\int_0^\infty \frac{\partial n}{\partial\tau}(t,\tau,\omega)\,\mathrm{d}\omega\right]\left[\phi_1(t,\tau)\mathbf{B}(t,\tau)+\phi_2(t,\tau)\mathbf{B}^2(t,\tau)\right]\mathrm{d}\tau,
$$

and the functions $\phi_1(t,\tau)$ and $\phi_2(t,\tau)$ read

$$
\begin{aligned}
\phi_1(t,\tau) &= \frac{\partial w}{\partial I_1}(I_1(\mathbf{C}(t,\tau)),I_2(\mathbf{C}(t,\tau)))+I_1(\mathbf{C}(t,\tau))\frac{\partial w}{\partial I_2}(I_1(\mathbf{C}(t,\tau)),I_2(\mathbf{C}(t,\tau))),\\
\phi_2(t,\tau) &= -\frac{\partial w}{\partial I_2}(I_1(\mathbf{C}(t,\tau)),I_2(\mathbf{C}(t,\tau))).
\end{aligned}
$$

By analogy with Eq. (16), we find from Eq. (14) that

$$
V(t) = 2\left[N_{\mathrm{p}}(t)+\int_0^\infty n(t,0,\omega)\,\mathrm{d}\omega\right]\boldsymbol{\Lambda}_0(t):\mathbf{D}(t),
\tag{17}
$$

where $\mathbf{\Lambda}_0(t) = \psi_1(t)\mathbf{B}_0(t) + \psi_2(t)\mathbf{B}_0^2(t)$, $\mathbf{B}_0(t)$ is the left Cauchy tensor for transition from the reference state to the deformed state at time t, and the functions $\psi_k(t)$ $(k = 1, 2)$ are given by

$$\psi_1(t) = \frac{\partial w}{\partial I_1}(I_1(\mathbf{C}_0(t)), I_2(\mathbf{C}_0(t))) + I_1(\mathbf{C}_0(t))\frac{\partial w}{\partial I_2}(I_1(\mathbf{C}_0(t)), I_2(\mathbf{C}_0(t))),$$
$$\psi_2(t) = -\frac{\partial w}{\partial I_2}(I_1(\mathbf{C}_0(t)), I_2(\mathbf{C}_0(t))).$$

It follows from Eqs. (13), (16) and (17) that

$$\frac{\mathrm{d}W}{\mathrm{d}t}(t) = 2\mathbf{H}(t) : \mathbf{D}(t) - Y(t) \tag{18}$$

with

$$\mathbf{H}(t) = \mathbf{\Lambda}(t) + \mathbf{\Lambda}_0(t)\left[N_{\mathrm{p}}(t) + \int_0^\infty n(t, 0, \omega)\,\mathrm{d}\omega\right].$$

For isothermal deformation of an incompressible medium, the Clausius–Duhem inequality reads

$$Q = -\frac{\mathrm{d}W}{\mathrm{d}t} + \frac{1}{\rho}\mathbf{\Sigma}' : \mathbf{D} \geqslant 0,$$

where ρ is mass density, $\mathbf{\Sigma}'$ is the deviatoric component of the Cauchy stress tensor $\mathbf{\Sigma}$, and Q is the internal dissipation per unit mass. Substitution of Eq. (18) into this equality results in

$$Q = \frac{1}{\rho}(\mathbf{\Sigma}' - 2\rho\mathbf{H}) : \mathbf{D} + Y \geqslant 0. \tag{19}$$

Because the function $Y(t)$ is non-negative, Eq. (19) is satisfied for an arbitrary deformation program, provided that the expression in brackets vanishes. This implies the constitutive equation

$$\mathbf{\Sigma}(t) = -P(t)\mathbf{I} + 2\rho\left\{\left[N_{\mathrm{p}}(t) + \int_0^\infty n(t, 0, \omega)\,\mathrm{d}\omega\right]\left[\psi_1(t)\mathbf{B}_0(t) + \psi_2(t)\mathbf{B}_0^2(t)\right] + \int_0^t\left[\int_0^\infty \frac{\partial n}{\partial \tau}(t, \tau, \omega)\,\mathrm{d}\omega\right]\left[\phi_1(t, \tau)\mathbf{B}(t, \tau) + \phi_2(t, \tau)\mathbf{B}^2(t, \tau)\right]\mathrm{d}\tau\right\}, \tag{20}$$

where P is pressure.

The stress–strain relation (20) is determined by the strain energy density $w(I_1, I_2)$, the rate of separation of active strands Γ_0 and the function N_{p} that determines mechanically induced activation of passive meso-regions. When $\Gamma_0 = 0$ and N_{p} is constant, Eq. (20) is transformed into the Finger formula for the Cauchy stress tensor in an isotropic and homogeneous hyperelastic solid. When both Γ_0 and N_{p} are constant, Eq. (20) is reduced to the BKZ constitutive equation (Bernstein et al., 1963) for a viscoelastic medium with a strain-independent relaxation spectrum. For a constant N_{p} and an attempt rate, Γ_0, dependent on the first two principal invariants of the relative right Cauchy tensor $\mathbf{C}$, Eq. (20) generalizes the Wagner equation (Wagner, 1976; Wagner et al., 1979) for the time-dependent behavior of polymeric melts. Finally, when both N_{p} and Γ_0 become functions of strain, Eq. (20) allows mechanically induced changes in the relaxation spectra and strengthening (weakening) of the viscoelastic response of elastomers to be predicted in a unified manner.

6. Uniaxial tension of a bar

Points of a bar refer to Cartesian coordinates $\{X_i\}$ in the stress-free state and to Cartesian coordinates $\{x_i\}$ in the deformed state, $(i = 1, 2, 3)$. Uniaxial tension of an incompressible medium is described by the formulas

$$x_1 = k(t)X_1, \quad x_2 = k^{-(1/2)}(t)X_2, \quad x_3 = k^{-(1/2)}(t)X_3,$$

where $k = k(t)$ is the extension ratio. The left Cauchy tensor, $\mathbf{B}_0(t)$, and the relative left Cauchy tensor, $\mathbf{B}(t,\tau)$, are given by

$$\begin{aligned} \mathbf{B}_0(t) &= k^2(t)\mathbf{e}_1\mathbf{e}_1 + \frac{1}{k(t)}(\mathbf{e}_2\mathbf{e}_2 + \mathbf{e}_3\mathbf{e}_3), \\ \mathbf{B}(t,\tau) &= \left(\frac{k(t)}{k(\tau)}\right)^2 \mathbf{e}_1\mathbf{e}_1 + \frac{k(\tau)}{k(t)}(\mathbf{e}_2\mathbf{e}_2 + \mathbf{e}_3\mathbf{e}_3), \end{aligned} \tag{21}$$

where $\mathbf{e}_i$ are base vectors of the frame $\{X_i\}$. To find the non-zero components Σ_k $(k = 1, 2)$ of the Cauchy stress tensor

$$\mathbf{\Sigma} = \Sigma_1\mathbf{e}_1\mathbf{e}_1 + \Sigma_2(\mathbf{e}_2\mathbf{e}_2 + \mathbf{e}_3\mathbf{e}_3),$$

we substitute of expressions (21) into Eq. (20) and exclude the unknown pressure, P, from the boundary condition $\Sigma_2 = 0$. The longitudinal stress $\sigma = \Sigma_1$ reads

$$\begin{aligned} \sigma(t) = 2\rho\Bigg\{ &\left[N_{\rm p}(t) + \int_0^\infty n(t,0,\omega)\,{\rm d}\omega\right]\left[\psi_1(t) + \psi_2(t)\left(k^2(t) + k^{-1}(t)\right)\right]\left[k^2(t) - k^{-1}(t)\right] \\ &+ \int_0^t \left[\int_0^\infty \frac{\partial n}{\partial \tau}(t,\tau,\omega)\,{\rm d}\omega\right]{\rm d}\tau\left[\phi_1(t,\tau) + \phi_2(t,\tau)\left(\left(\frac{k(t)}{k(\tau)}\right)^2 + \frac{k(\tau)}{k(t)}\right)\right]\left[\left(\frac{k(t)}{k(\tau)}\right)^2 - \frac{k(\tau)}{k(t)}\right]\Bigg\}. \end{aligned} \tag{22}$$

To compare results of numerical simulation with the experimental data, we focus on a standard relaxation test with

$$k(t) = \begin{cases} 1, & t < 0, \\ \lambda, & t > 0, \end{cases} \tag{23}$$

where $\lambda > 1$ is a constant. Substitution of Eq. (23) into Eq. (22) results in the following expression for the engineering stress $\sigma_{\rm e} = \sigma/\lambda$:

$$\sigma_{\rm e}(t,\lambda) = 2\rho\left[N_{\rm p}(\lambda) + \int_0^\infty n(t,0,\omega)\,{\rm d}\omega\right]\left[\psi_1(\lambda) + \psi_2(\lambda)(\lambda^2 + \lambda^{-1})\right](\lambda - \lambda^{-2}), \tag{24}$$

where the quantities $N_{\rm p}$, ψ_1 and ψ_2 become functions of the elongation ratio λ. It follows from Eqs. (1), (2) and (7) that for the deformation program (23), the function $n(t,0,\omega)$ reads

$$n(t,0,\omega) = N_{\rm a}(\lambda)\exp[-\Gamma_0(\lambda)\exp(-\omega)t]p(\omega).$$

This equality together with Eqs. (1) and (24) implies that

$$\sigma_{\rm e}(t,\lambda) = \sigma_0(\lambda)\left\{1 - \kappa(\lambda)\int_0^\infty [1 - \exp(-\Gamma_0(\lambda)\exp(-\omega)t)]p(\omega)\,{\rm d}\omega\right\}, \tag{25}$$

where

$$\sigma_0(\lambda) = 2\rho N\big[\psi_1(\lambda) + \psi_2(\lambda)\big(\lambda^2 + \lambda^{-1}\big)\big](\lambda - \lambda^{-2}), \quad \kappa(\lambda) = \frac{N_a(\lambda)}{N}. \tag{26}$$

To fit experimental data, we adopt the random energy model (Derrida, 1980) for the distribution of active meso-regions with various activation energies

$$p(\omega) = p_0 \exp\left[-\frac{(\omega - \Omega)^2}{2\Sigma^2}\right] \quad \omega \geqslant 0, \qquad p(\omega) = 0 \quad \omega < 0, \tag{27}$$

where Ω and Σ are adjustable parameters of the quasi-Gaussian probability density, and the constant p_0 is determined by the condition

$$\int_0^\infty p(\omega)\,\mathrm{d}\omega = 1. \tag{28}$$

To rationalize the choice of the distribution function (27), we refer to the fact that (according to the central limit theorem) the cumulative effect of a large number of independent random factors may be adequately described by a Gaussian distribution. Among these factors, we would mention different types of junctions between chain ends, adsorption of chains to surfaces of filler particles, segregation of short chains to clusters of particles, formation of physical cross-links between macromolecules in the elastomeric matrix, mechanically induced transformations of chemical cross-links, etc.

Given an elongation ratio, λ, Eqs. (25) and (27) are determined by five material constants:

1. the apparent average potential energy for separation of strands from temporary junctions Ω,
2. the apparent standard deviation of potential energies for detachment of strands in active meso-regions Σ,
3. the attempt rate for separation of active strands from temporary nodes Γ_0,
4. the concentration of active meso-domains κ,
5. the stress at the beginning of the relaxation process σ_0.

The number of experimental constants in Eqs. (25) and (27) is quite comparable with that in phenomenological stress–strain relations conventionally employed to fit observations in relaxation tests (based on the generalized Maxwell model with several relaxation times, on the stretched exponential function, or on the rheological modes with fractional derivatives). An advantage of Eqs. (25) and (27) is that the adjustable parameters have a transparent physical meaning (unlike the orders of fractional derivatives in fractional differential equations or the exponent in the Kohlrausch–Williams–Watt function).

Our aim now is to find the adjustable parameters by matching the relaxation curves depicted in Figs. 1–3.

7. Fitting of experimental data

Eqs. (25) and (27) imply that

$$\sigma_e(t,\lambda) = C_1(\lambda) + p_0 C_2(\lambda)\int_0^\infty [1 - \exp(-\Gamma_0(\lambda)\exp(-\omega)t)]\exp\left[-\frac{(\omega-\Omega)^2}{2\Sigma^2}\right]\mathrm{d}\omega, \tag{29}$$

where

$$C_1(\lambda) = \sigma_0(\lambda), \quad C_2(\lambda) = -\sigma_0(\lambda)\kappa(\lambda). \tag{30}$$

It follows from Eq. (29) that the attempt rate, Γ_0, and the apparent average potential energy, Ω, are mutually dependent. Indeed, an increase in Ω by $\delta\Omega$ induces shift $\omega \to \omega + \delta\Omega$ of activation energies, which

is tantamount by the replacement of Γ_0 by $\Gamma_0 \exp(\delta\Omega)$ in Eq. (29). For definiteness, we choose some elongation ratio, $\lambda = \lambda_k$, for any rubber compound and set $\Gamma_0(\lambda_k) = 1$ s in the approximation of experimental data.

First, we match the relaxation curves for rubber compound R1. We begin with fitting the experimental data measured at the elongation ratio $\lambda_1 = 2.0$. Under the condition $\Gamma_0(\lambda_1) = 1$ s, the relaxation curve is determined by 4 experimental constants, Ω, Σ, C_1 and C_2. To find these quantities, we fix some intervals, $[0, \Omega_{\max}]$ and $[0, \Sigma_{\max}]$, where the "best-fit" parameters Ω and Σ are assumed to be located, and divide these intervals into J subintervals by the points $\Omega_i = i\Delta_\Omega$ and $\Sigma_j = j\Delta_\Sigma$ $(i, j = 1, \ldots, J)$ with $\Delta_\Omega = \Omega_{\max}/J$, $\Delta_\Sigma = \Sigma_{\max}/J$. For any pair, $\{\Omega_i, \Sigma_j\}$, we evaluate the integral in Eq. (29) numerically (by Simpson's method with 200 points and the step $\Delta_\omega = 0.2$). The pre-factor p_0 is found from Eq. (28). The coefficients $C_1 = C_1(i, j)$ and $C_2 = C_2(i, j)$ are calculated by the least-squares method from the condition of minimum of the function

$$\mathscr{J}(i, j) = \sum_{t_m} \left[\sigma_{\exp}(t_m) - \sigma_{\text{num}}(t_m)\right]^2, \tag{31}$$

where the sum is taken over all experimental points t_m. The stress $\sigma_{\exp}$ in Eq. (31) is the engineering stress measured in the relaxation test, whereas the stress σ_{num} is given by Eq. (29). The best-fit parameters Ω and Σ minimize the function $\mathscr{J}$ on the set $\{\Omega_i, \Sigma_j \ (i, j = 1, \ldots, J)\}$. After determining the best-fit values, Ω_i and Σ_j, we repeat this procedure for the new intervals $[\Omega_{i-1}, \Omega_{i+1}]$ and $[\Sigma_{j-1}, \Sigma_{j+1}]$ to ensure an acceptable accuracy of fitting.

To match the relaxation curves at higher elongation ratios, λ_k, we fix the constants Ω and Σ found by fitting observations at λ_1 and approximate any relaxation curve by using three adjustable parameters, Γ_0, C_1 and C_2. These quantities are determined by an algorithm similar to that employed in the approximation of the relaxation curve at λ_1. We fix an interval $[0, \Gamma_{\max}]$, where the best-fit attempt rate Γ_0 is supposed to be located, and divide this interval into J subintervals by the points $\Gamma_i = i\Delta_\Gamma$ $(i = 1, \ldots, J)$ with $\Delta_\Gamma = \Gamma_{\max}/J$. For any Γ_i, we evaluate the integral in Eq. (29) numerically and find the coefficients $C_1 = C_1(i)$ and $C_2 = C_2(i)$ (that minimize the function (31)) by the least-squares method. The best-fit attempt rate minimizes the function $\mathscr{J}$ on the set $\{\Gamma_i (i = 1, \ldots, J)\}$. After finding this best-fit value, Γ_i, the procedure is repeated for the new interval $[\Gamma_{i-1}, \Gamma_{i+1}]$ to provide an acceptable accuracy of the approximation. Fig. 1 demonstrates fair agreement between the experimental data and the results of numerical simulation with $\Omega = 6.66$ and $\Sigma = 10.12$ at all elongation ratios.

The same procedure is applied to approximate the relaxation curves for specimens R2 and R3. The only difference is that we use the step $\Delta_\omega = 0.08$ to evaluate the integral in Eq. (29) and begin matching observations from the relaxation curve measured at the maximum elongation ratio $\lambda_4 = 3.5$ (which means that we postulate $\Gamma_0(\lambda_4) = 1$ s). The best-fit parameters Ω and Σ read 6.27 and 5.68 for samples R2 and 7.06 and 4.44 for specimens R3, respectively. Figs. 2 and 3 show good correspondence between the observations and the results of numerical analysis.

For the distribution function (27), the parameters Ω and Σ do not coincide with the average potential energy for detachment of active strands, Ω_0, and the standard deviation of potential energies for separation of strands from the network, Σ_0. The latter quantities read

$$\Omega_0 = \int_0^\infty \omega p(\omega)\, \mathrm{d}\omega, \quad \Sigma_0 = \left[\int_0^\infty (\omega - \Omega_0)^2 p(\omega)\, \mathrm{d}\omega\right]^{1/2}. \tag{32}$$

The dimensionless parameters Ω_0, Σ_0 and $\xi = \Sigma_0/\Omega_0$ given by Eq. (32) are listed in Table 1, which shows that the width of the quasi-Gaussian distribution (characterized by the ratio ξ) changes rather weakly.

For any elongation ratio, λ_k, the attempt rate, $\Gamma_0(\lambda_k)$, is determined by matching an appropriate relaxation curve. The fraction of active meso-domains, $\kappa(\lambda_k)$, is found from Eq. (30),

$$\kappa(\lambda_k) = -\frac{C_2(\lambda_k)}{C_1(\lambda_k)}.$$

Table 1
Adjustable parameters Ω_0, Σ_0 and ξ

Sample	Ω_0	Σ_0	ξ
R1	10.96	7.34	0.67
R2	7.11	3.99	0.56
R3	7.34	3.68	0.50

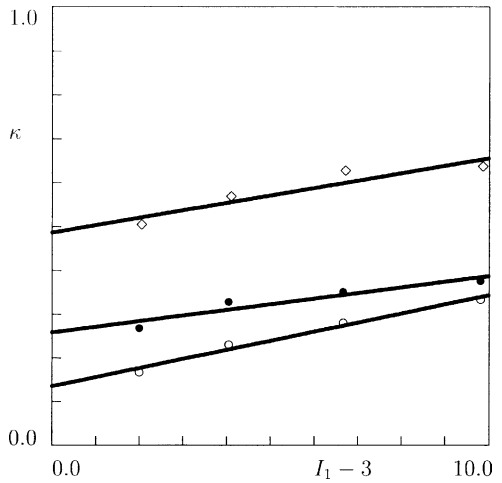

Fig. 4. The concentration of active meso-regions κ versus the first invariant I_1 of the right Cauchy tensor. Symbols: treatment of observations. (♢) R1; (○) R2; (●) R3. (—) approximation of the experimental data by Eq. (33).

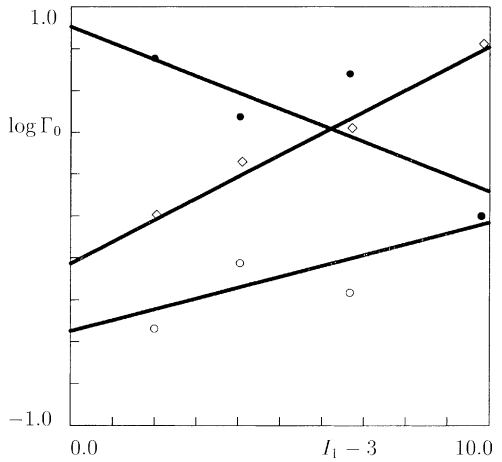

Fig. 5. The attempt rate Γ_0 s^{-1} versus the first invariant I_1 of the right Cauchy tensor. Symbols: treatment of observations. (♢) R1; (○) R2; (●) R3. (—) approximation of the experimental data by Eq. (33).

These quantities are plotted in Figs. 4 and 5 versus the first invariant, $I_1 = \lambda^2 + 2\lambda^{-1}$, of the right Cauchy tensor $\mathbf{C}_0$. The experimental data are fitted by the phenomenological equations

Table 2
Adjustable parameters a_0, a_1, b_0 and b_1

Sample	a_0	a_1	b_0	b_1
R1	0.49	0.017	−0.23	0.104
R2	0.14	0.021	−0.55	0.052
R3	0.26	0.013	0.91	−0.079

$$\kappa = a_0 + a_1(I_1 - 3), \quad \log \Gamma_0 = b_0 + b_1(I_1 - 3), \tag{33}$$

where the coefficients a_i and b_i ($i = 0, 1$) are found by the least-squares method. Figs. 4 and 5 show an acceptable agreement between the observations and their approximations by Eq. (33) with the parameters a_i and b_i collected in Table 2. The choice of the amount $I_1 - 3$ in the presentation of experimental data in Figs. 4 and 5 may be explained by the fact that this quantity is proportional to the mechanical energy of an elastomeric network within the classical theory of rubber elasticity (Kloczkowski, 2002).

8. Discussion

Figs. 1–3 reveal good agreement between the measured relaxation curves and the results of numerical simulation based on the assumption that the distribution function of meso-domains with various activation energies, $p(\omega)$, is strain independent. Because this function characterizes the relaxation spectrum of specimens, we conclude that the distribution of relaxation times for filled rubbers under investigation is independent of mechanical factors.

According to Table 1, the relaxation times are weakly affected by the content of filler. The three-fold growth of the fraction of carbon black (from 20 to 60 phr) implies an increase in the average potential energy for detachment of strands by 3% and a decrease in the width of the distribution of potential energies by 11%.

Fig. 4 demonstrates that the concentration of active meso-regions, where rearrangement of strands occurs, monotonically grows with elongation ratio. With reference to Table 2, we conclude that the initial fraction of active meso-domains strongly depends on the chemical formulation of rubber compounds (the parameter a_0 varies from 0.14 to 0.49). For the same chemical composition of a particle-reinforced elastomer, it noticeably increases with filler content (from 0.14 at 20 phr to 0.26 at 60 phr of carbon black). This conclusion is in agreement with observations by Aksel and Hübner (1996) which revealed that an increase in the volume fraction of filler dramatically enhanced stress relaxation. The coefficient a_1 that describes the effect of stretching on the concentration of active meso-domains weakly depends on composition of the rubber compounds. A decrease in a_1 is observed with the growth of the filler content (from 0.021 for specimens R2 to 0.013 for samples R3), which may be explained by the influence of the secondary network of filler in rubber R3 that prevents mechanically induced activation of passive meso-regions.

Fig. 5 shows that the attempt rate, Γ_0, increases with elongation ratio for specimens R1 and R2. The growth of the attempt rate is in agreement with the free volume concept (Knauss and Emri, 1987; Losi and Knauss, 1992; O'Dowd and Knauss, 1995), which ascribes an increase in the relaxation rate with strain to an increase in the free volume per macromolecule (that, in turn, enhances molecular mobility). The effect of stretching on the attempt rate is characterized by the coefficient a_1 that accepts similar values (0.104 for R1 and 0.052 for R2) for the two grades of particle-reinforced rubbers. In contrast, the attempt rate for specimens R3 decreases with strain. The difference in the influence of mechanical factors on the attempt rate for specimens R2 and R3 may be attributed to the presence of a secondary network of filler in rubber compound R3.

Comparison of Figs. 2 and 3 shows that the formation of the secondary network in compound R3 implies a substantial growth of stress, which means that this secondary network carries out a large part of the applied load. Under stretching, a part of the secondary network is fragmented into pieces (individual particles and small clusters of filler), which serve as extra physical cross-links in active meso-regions. These cross-links resist separation of active chains from temporary nodes, which results in slowing down of the rearrangement process.

9. Comparison with other models

The scenario for the viscoelastic response of particle-reinforced elastomers proposed in this study is based on the following hypotheses:

1. Filled rubber may be treated as an ensemble of meso-regions that are rearranged independently of each other.
2. The rearrangement process is thermally activated, and its rate obeys by the Eyring equation.
3. Mechanical factors affect the distribution of meso-domains with various potential energies, which is reflected by activation of passive meso-regions.

Our purpose now is to compare these assumptions with postulates employed in other models for the time-dependent behavior of disordered media, where relaxation of stresses is associated with rearrangement of structural units. In this analysis we disregard the physical nature of relaxing units (which is different for elastomers and, for example, structural glasses) and concentrate on the kinetics of rearrangement exclusively.

In the Gilroy–Phillips (GP) model (Gilroy and Phillips, 1981; Buchenau, 2001), the viscoelastic response of a glass is attributed to hops of flow units (trapped in potential wells on the energy landscape) from one minimum of a double-well potential to another over an energy barrier. The hops are driven by thermal fluctuations, whereas the depths of the asymmetric wells are assumed to be strain dependent. An ensemble of potential wells is entirely described by the distribution of heights of energy barriers (similar to the distribution function, $p(\omega)$, for meso-regions with various activation energies) and by an analog of the Eyring formula (2) for the rate of hops over energy barriers. For a uniaxial relaxation test with small strains (which corresponds to the case when mechanically induced activation of passive meso-domains is prevented), Eq. (14) of Buchenau (2001) coincides with Eq. (25) of the present work, where κ and Γ_0 are taken to be strain independent. However, for more complicated deformation programs (three-dimensional loadings or one-dimensional loadings with finite strains), the GP concept fails to predict the mechanical response, because no information is available on how the double-well potential is affected by the strain tensor.

According to a soft glassy rheology (SGR) model (Sollich et al., 1997; Sollich, 1998; Fiedling et al., 2000), a disordered medium is treated as an ensemble of relaxing units located in potential wells (with various depths) on the energy landscape. Under loading, any unit rises from the bottom of its potential well to a higher energy level (which is proportional to the strain energy stored by the unit). The viscoelastic response is associated with thermally activated hops of relaxing regions in their potential wells. When a unit reaches some liquid-like energy level, it is rearranged (which means that it accepts the current state of a deformed medium as its new reference state) and it randomly chooses a new potential well on the energy landscape to be trapped. Evolution of the concentration of relaxing units located in cages with various potential energies is described by the Bouchaud equation (Bouchaud, 1992) appropriately modified to account for the effect of mechanical energy on the rate of rearrangement of relaxing elements. A disadvantage of the SGR concept is that it implies a nonlinear viscoelastic response even at very small strains,

whereas elastomers demonstrate the linear time-dependent behavior at relatively small deformations. Another shortcoming of this approach is that the SGR model implies changes in the population of traps with various potential energies (mechanically induced aging of a disordered material), whose rates are comparable with the characteristic rate of stress relaxation (the latter is not confirmed by observations on rubbery polymers).

Finally, it is worth mentioning some similarities between our scenario for strain-induced activation of passive meso-regions in filled elastomers and a version of the concept of transient networks proposed by Wang (1992) and Ahn and Osaki (1995) to predict shear thickening of polymeric solutions. The difference between the two approaches is that in the Wang model, deformation of a polymeric medium results in merging of chains with two free ends with a transient network, whereas, according to our concept, strands (that were permanent in the stress-free state) begin to separate from temporary nodes under loading.

10. Concluding remarks

Relaxation curves have been reported for three commercial grades of CB-filled natural rubber in tensile relaxation tests at room temperature. A constitutive model has been derived for the nonlinear viscoelastic response of particle-reinforced elastomers at finite strains. A complicated micro-structure of filled rubber is modelled as an equivalent transient network of macromolecules. The network is assumed to be strongly heterogeneous, and it is treated as an ensemble of meso-regions with various activation energies for separation of strands from temporary nodes. Two types of meso-domains are introduced: passive, where rearrangement of strands is prevented by surrounding chains and filler clusters, and active, where the rearrangement process is governed by the Eyring equation. Deformation of a rubber compound (i) leads to activation of passive meso-regions and (ii) alters the attempt rate for detachment of active strands from the network. Adjustable parameters in the stress–strain relations are found by fitting observations in relaxation tests at elongations up to 350%. Fair agreement is demonstrated between the experimental data and the results of numerical simulation. The following conclusions are drawn:

1. The random energy model with strain-independent parameters Ω and Σ ensures fair agreement between the observations and the results of numerical simulation. The average activation energy for detachment of active chains from temporary junctions is strongly affected by the chemical formulation of rubber compounds, whereas the width of the quasi-Gaussian distribution function (27) weakly changes with the filler content.
2. Stretching of specimens results in mechanically induced activation of passive meso-regions. The concentration of active meso-domains linearly increases with the first invariant of the right Cauchy tensor. The rate of growth of κ decreases with the content of particles, which is attributed to the influence of the secondary network of filler that resists activation of passive domains.
3. At low concentrations of filler, the attempt rate exponentially grows with the first invariant of the right Cauchy tensor. This increase is ascribed to the growth of the free volume per macromolecule that enhances molecular mobility. When the content of particles exceeds the percolation threshold, the attempt rate for separation of strands from temporary nodes decreases with elongation ratio, which may be explained by fragmentation of the secondary network of filler into individual particles and small clusters which serve as extra cross-links in active meso-domains.

It should be noted that some important questions remained beyond the scope of the present work. In particular, the effects of (i) a test's temperature, (ii) aggregation of CB particles, and (iii) interactions between CB clusters and the host matrix on the viscoelastic behavior of a particle-reinforced elastomer have not been analyzed in detail. These issues will be the subject of subsequent studies. An attempt to analyze the

influence of temperature on the viscoelastic behavior of a transient polymeric network has recently been undertaken in Drozdov and Christiansen (2002).

References

Ahn, K.H., Osaki, K., 1995. Mechanism of shear thickening investigated by a network model. Journal of Non-Newtonian Mechanics 56, 267–288.

Aksel, N., Hübner, Ch., 1996. The influence of dewetting in filled elastomers on the changes of their mechanical properties. Archive of Applied Mechanics 66, 231–241.

Arruda, E.M., Boyce, M.C., Jayachandran, R., 1995. Effects of strain rate, temperature and thermomechanical coupling on the finite strain deformation of glassy polymers. Mechanics of Materials 19, 193–212.

Bergström, J.S., Boyce, M.C., 1998. Constitutive modelling of the large strain time-dependent behavior of elastomers. Journal of the Mechanics and Physics of Solids 46, 931–954.

Bergström, J.S., Kurtz, S.M., Rimnac, C.M., Edidin, A.A., 2002. Constitutive modeling of ultra-high molecular weight polyethylene under large-deformation and cyclic loading conditions. Biomaterials 23, 2329–2343.

Bernstein, B., Kearsley, E.A., Zapas, L.J., 1963. A study of stress relaxation with finite strains. Transactions of the Society of Rheology 7, 391–410.

Bouchaud, J.P., 1992. Weak ergodicity breaking and aging in disordered systems. Journal de Physique I 2, 1705–1713.

Boukamel, A., Meo, S., Debordes, O., Jaeger, M., 2001. A thermo-viscoelastic model for elastomeric behaviour and its numerical application. Archive of Applied Mechanics 71, 785–801.

Boyce, M.C., Arruda, E.M., 2000. Constitutive models of rubber elasticity: a review. Rubber Chemistry and Technology 73, 504–523.

Buchenau, U., 2001. Mechanical relaxation in glasses and at the glass transition. Physical Review B 63, 104–203.

Carlier, V., Sclavons, M., Jonas, A.M., Jerome, R., Legras, R., 2001. Probing thermoplastic matrix-carbon interphases. 1. Preferential segregation of low molar mass chains to the interface. Macromolecules 34, 3725–3729.

Choi, S.-S., 1998. Influence of silica content on migration of antidegradants to the surface in NR vulcanizates. Journal of Applied Polymer Science 68, 1821–1828.

Choi, S.-S., 2002. Strain and anisotropic effects on migration behaviors of antiozonants in carbon black-filled natural rubber vulcanizates. Polymer Testing 21, 741–744.

Clarke, S.M., Elias, F., Terentjev, E.M., 2000. Ageing of natural rubber under stress. European Physical Journal E 2, 335–341.

Derrida, B., 1980. Random-energy model: limit of a family of disordered models. Physical Review Letters 45, 79–92.

Drozdov, A.D., 1996. Finite Elasticity and Viscoelasticity. World Scientific, Singapore.

Drozdov, A.D., 1997. A constitutive model for nonlinear viscoelastic media. International Journal of Solids and Structures 34, 2685–2707.

Drozdov, A.D., Christiansen, J.deC., 2002. The effect of annealing on the time-dependent behavior of isotactic polypropylene at finite strains. Polymer 43, 4745–4761.

Drozdov, A.D., Dorfmann, A., 2002. Finite viscoelasticity of filled rubbers: the effects of pre-loading and thermal recovery. Continuum Mechanics and Thermodynamics 14, 337–361.

Eyring, H., 1936. Viscosity, plasticity, and diffusion as examples of absolute reaction rates. Journal of Chemical Physics 4, 283–291.

Fiedling, S.M., Sollich, P., Cates, M.E., 2000. Aging and rheology of soft materials. Journal of Rheology 44, 323–369.

Gilroy, K.S., Phillips, W.A., 1981. An asymmetric double-well potential model for structural relaxation processes in amorphous materials. Philosophical Magazine B 43, 735–746.

Green, M.S., Tobolsky, A.V., 1946. A new approach to the theory of relaxing polymeric media. Journal of Chemical Physics 14, 80–92.

Ha, K., Schapery, R.A., 1998. A three-dimensional viscoelastic constitutive model for particulate composites with growing damage and its experimental validation. International Journal of Solids and Structures 35, 3497–3517.

Haupt, P., Sedlan, K., 2001. Viscoplasticity of elastomeric materials: experimental facts and constitutive modelling. Archive of Applied Mechanics 71, 89–109.

Holzapfel, G., Simo, J., 1996. A new viscoelastic constitutive model for continuous media at finite thermomechanical changes. International Journal of Solids and Structures 33, 3019–3034.

Inberg, J.P.F., Takens, A., Gaymans, R.J., 2002. Strain rate effects in polycarbonate and polycarbonate/ABS blends. Polymer 43, 2795–2802.

Jung, G.D., Youn, S.K., Kim, B.K., 2000. A three dimensional nonlinear constitutive model of solid propellant. International Journal of Solids and Structures 37, 4715–4732.

Karasek, L., Sumita, M., 1996. Characterization of dispersion state of filler and polymer-filler interactions in rubber-carbon black composites. Journal of Materials Science 31, 281–289.

Kim, B.-K., Youn, S.-K., 2001. A viscoelastic constitutive model of rubber under small oscillatory load superimposed on large static deformation. Archive of Applied Mechanics 71, 748–763.

Kloczkowski, A., 2002. Application of statistical mechanics to the analysis of various physical properties of elastomeric networks—a review. Polymer 43, 1503–1525.

Knauss, W.G., Emri, I.J., 1987. Volume change and the nonlinearly thermoviscoelastic constitution of polymers. Polymer Engineering and Science 27, 86–100.

Lion, A., 1996. A constitutive model for carbon black filled rubber: experimental investigations and mathematical representation. Continuum Mechanics and Thermodynamics 8, 153–169.

Lion, A., 1997. On the large deformation behavior of reinforced rubber at different temperatures. Journal of the Mechanics and Physics of Solids 45, 1805–1834.

Lion, A., 1998. Thixotropic behaviour of rubber under dynamic loading histories: experiments and theory. Journal of the Mechanics and Physics of Solids 46, 895–930.

Losi, G.U., Knauss, W.G., 1992. Free volume theory and nonlinear thermoviscoelasticity. Polymer Engineering and Science 32, 542–557.

Mandal, U.K., Aggarwal, S., 2001. Studies on rubber-filler interaction in carboxylated nitrile rubber through microhardness measurement. Polymer Testing 20, 305–311.

Miehe, C., Keck, J., 2000. Superimposed finite elastic–viscoelastic–plastoelastic stress response with damage in filled rubbery polymers. Experiments, modelling and algorithmic implementation. Journal of the Mechanics and Physics of Solids 48, 323–365.

O'Dowd, N.P., Knauss, W.G., 1995. Time dependent large principal deformation of polymers. Journal of the Mechanics and Physics of Solids 43, 771–792.

Reese, S., Govindjee, S., 1998. Theoretical and numerical aspects in the thermo-viscoelastic material behaviour of rubber-like polymers. Mechanics of Time-Dependent Materials 1, 357–396.

Septanika, E.G., Ernst, L.J., 1998a. Application of the network alteration theory for modeling the time-dependent constitutive behaviour of rubbers. 1. General theory. Mechanics of Materials 30, 253–263.

Septanika, E.G., Ernst, L.J., 1998b. Application of the network alteration theory for modeling the time-dependent constitutive behaviour of rubbers. 2. Further evaluation of the general theory and experimental verification. Mechanics of Materials 30, 265–273.

Sollich, P., 1998. Rheological constitutive equation for a model of soft glassy materials. Physical Review E 58, 738–759.

Sollich, P., Lequeux, F., Hebraud, P., Cates, M.E., 1997. Rheology of soft glassy materials. Physical Review Letters 78, 2020–2023.

Spathis, G., 1997. Non-linear constitutive equations for viscoelastic behaviour of elastomers at large deformations. Polymer Gels and Networks 5, 55–68.

Tanaka, F., Edwards, S.F., 1992. Viscoelastic properties of physically cross-linked networks. Transient network theory. Macromolecules 25, 1516–1523.

Wagner, M.H., 1976. Analysis of time-dependent non-linear stress-growth data for shear and elongation flow of a low-density branched polyethylene melts. Rheologica Acta 15, 136–142.

Wagner, M.H., Raible, T., Meissner, J., 1979. Tensile stress overshoot in uniaxial extension of a LDPE melt. Rheologica Acta 18, 427–428.

Wang, S.-Q., 1992. Transient network theory for shear-thickening fluids and physically cross-linked systems. Macromolecules 25, 7003–7010.

Wu, J.-D., Liechti, K.M., 2000. Multiaxial and time dependent behavior of a filled rubber. Mechanics of Time-Dependent Materials 4, 293–331.

Yamamoto, M., 1956. The visco-elastic properties of network structure. 1. General formalism. Journal of the Physical Society of Japan 11, 413–421.